Mitochondrial Activity Regulates Skin-derived Mesenchymal Stem Cell Differentiation Into Brown Adipocyte Contributing to Hypertension

Da Wen Xi
Shanghai Institute of Hypertention
Dong Wen Chen
Shanghai Institute of Hypertension
Hong Wei Sun
Henan University Digestive Institute
Xiao Xiang Li
Shanghai Institute of Hypertension
Min Zhi Suo
Henan University Digestive Institute
QUN LI (liqun@sibs.ac.cn)
Shanghai Institute of Hypertension https://orcid.org/0000-0002-0549-1852
Jin Ping Gao
Shanghai Institute of Hypertension

Research

Keywords: Skin-Derived Mesenchymal Stem Cell, Differentiation, Brown Adipocyte, Mitochondrial Activity, Hypertension

Posted Date: November 13th, 2020

DOI: https://doi.org/10.21203/rs.3.rs-105303/v1

Version of Record: A version of this preprint was published on March 10th, 2021. See the published version at https://doi.org/10.1186/s13287-021-02169-0.

Abstract

Background: Brown adipocytes (BAs) are the major component of brown adipose tissue (BAT) that is closely related to systemic hypertension. BAs are derived from multiple progenitors including PDGFRα$^+$ adipose-derived stem cells (ASCs). Skin-derived Mesenchymal Stem Cells (S-MSCs) have the capacity to differentiate into adipocytes. However, the differentiation of S-MSCs into BAs remains unexplored. We aim to study the ability and regulation mechanism of S-MSCs differentiation into BAs, and the direct role of BAT in blood pressure regulation.

Methods: Protein expression was measured by Flow Cytometry or Western blotting, and gene mRNA levels were detected by real-time quantitative PCR (RT-PCR). For the BA differentiation of S-MSCs, S-MSCs were stimulated with a brown adipogenic cocktail containing insulin, IBMX, dexamethasone, triiodothyronine (T3), and rosiglitazone for the indicated periods. The oxygen consumption rate (OCR) was measured with an XF24 Extracellular Flux Analyzer. Mitochondrial mass was checked by flow cytometry and fluorescence staining. Hypertensive mouse model was induced in WT mice by infusion with angiotensin II (Ang II) and measured SBP using tail-cuff. The interscapular brown adipose tissue (iBAT)-deficiency mice were gotten by surgically removing the iBAT depot and allowed to recover for 6 days. Aorta, iBAT or heart tissue sections were examined by hematoxylin and eosin (HE) staining.

Results: We found that S-MSCs isolated from the mouse dermis expressed the stem cell markers CD90/105 and PDGFRα, and readily differentiated into BAs. Mitochondrial biogenesis and oxygen consumption were markedly increased during BA differentiation of S-MSCs *in vitro.* Another, Ang II-induced hypertensive mice carried the change of iBAT to white adipose tissue (WAT), the enhanced Ang II-induced blood pressure and vascular remodeling were observed in BAT-deficient mice generated by surgically removing iBAT comparing with C57BL/6 (wild type-WT) mice.

Conclusions: S-MSCs represent a useful *in vitro* model for differentiation of BAs regulated by mitochondrial activity, and are progenitors of BAs. This study indicates that PDGFRα$^+$ S-MSCs could differentiate into BAs, and BAT plays a direct role in Ang II-induced hypertension and target organ remodeling.

Highlight

PDGFRα$^+$ S-MSCs are progenitors of BAs.

The process of S-MSCs differentiating into BAs was regulated by mitochondrial activity.

Brown adipose tissue deficiency aggravates Ang II-induced hypertension and target organs remodeling.

Background

The adipose organ is composed of WAT and BAT. WAT serves as an energy store for the body, whereas BAT utilizes chemical energy through uncoupled respiration and thermogenesis in all mammals [1]. BAT plays a critical role in energy homeostasis and body weight control via fat thermogenesis and is highly metabolically active, raising the possibility that it may serve as a potential therapeutic target for metabolic diseases [2]. Transgenic ablation of BAT is associated with not only obesity but also systemic hypertension and cardiac fibrosis as shown in transgenic mice with reduced brown fat [3, 4]. Fibroblast growth factor 21 (FGF21) derived from BAT plays an endocrine protective role against hypertensive cardiac remodeling in mice [5]. BAs are the major component of BAT and arise from distinct developmental origins, including adipogenic progenitors, myogenic factor 5 $(Myf5)^+$ progenitors and neuronal cell differentiation [6, 7]. However, the underlying origin of BAs is not completely understood.

Mesenchymal stem cells (MSCs) can be expanded and differentiated into a variety of mesenchymal cell types such as adipocytes, osteoblasts and chondrocytes [8]. Human fetal mesenchymal stem cells (fMSCs) have been shown to differentiate into BAs [9]. Previous studies have demonstrated that the $PDGFR\alpha^+$ ASCs isolated from WAT could differentiate into BAs *in vitro* and *in vivo* [10]. S-MSCs isolated from the largest lymphoid organ-skin, share functional similarities to MSCs and consistently differentiate into adipocytes, osteocytes, and chondrocytes as well [11, 12]. S-MSCs have the ability to migrate to the inflamed tissues and perform immunosuppressive activity to inhibit the development of atherosclerosis, EAE and hypertension in mouse models, which indicate that S-MSCs represent a promising cell source for stem cell-based therapies of chronic inflammatory diseases and possibly transplantation [12–15]. However, it is unknown whether S-MSCs can differentiate into BAs. Understanding of the specific mechanisms that regulate the differentiation of S-MSCs into BAs is very important to the development feasible clinical treatments.

Recent studies demonstrate that mitochondrial regulation is increasingly recognized as an important determining factor in stem cell biology and function. There has been mounting evidence that mitochondrial metabolism is implicated in the adipogenic differentiation of MSCs [16, 17]. In addition, the differentiation and homeostatic function of the adipose tissue are supported by mitochondrial biogenesis [18]. It is also worthwhile to note that BAs are rich in mitochondrial content, and the BAT has been known to play important roles in lipid metabolism and energy expenditure, with a rich expression of thermogenic markers which participate significantly in mitochondrial biogenesis [19, 20]. Studies have demonstrated that mitochondria play an important regulatory role in determining the differentiation capacity of MSCs [17].

Skin provides an easily accessible and ideal source of tissue for the isolation of S-MSCs. Thus far, no study has reported whether the S-MSCs located in the dermis can differentiate into BAs, or the effect of mitochondrial biogenesis and activity during the BA differentiation of S-MSCs. In our study, we demonstrated that S-MSCs readily differentiated into BAs regulated by mitochondrial activity, and the iBAT directly contributed to improving the blood pressure in Ang II-induced hypertensive mice.

Methods

Mice

C57BL/6J (WT) mice (8–12 weeks of age) were purchased from Shanghai SLAC Laboratory Animal Co. (Shanghai, China). All mice were kept under specific pathogen-free (SPF) conditions in compliance with the National Institutes of Health Guide for the Care and Use of Laboratory Animals with the approval (SYXK-2003-0026) of the Scientific Investigation Board of Shanghai Jiao Tong University School of Medicine, Shanghai, China.

Brown adipocytes differentiation of S-MSCs

Preparation, culture and characterization of S-MSCs were performed as described previously [12]. For *in vitro* BAs differentiation, S-MSCs were plated in complete medium at a density of 2×10^4 cells per square centimeter in 6-well culture plates and re-fed every 2 days until they were 100% confluent or post confluent. BAs differentiation was induced by treating cells for 48 hours in medium containing 10% FBS, 0.5 mM isobuylmethylxanthine (IBM), 1 μM dexamethasone (DEX), 240 IU/μM insulin, 1 nM T3 and 1 μM rosiglitazone (Alexis Biochemicals). After 48 hours, cells were switched to medium containing 10% FBS (Gibco, #10099-141, Australia), 240 IU/μM insulin, 1 nM T3 and 1 μM rosiglitazone for another 6–8 days, and the differentiation medium was replaced every 2 days. Images of cells were obtained at 0, 2, 4, 6, 8, and 10 days after stimulation by light microscopy (Zeiss, Germany). Original magnifications 100x or 400x.

Oxygen Consumption

S-MSCs were seeded at a density of 4×10^4 cells per well in XF 96-well plates. After BAs induction, OCR was detected with a Seahorse XF96 Extracellular Flux Analyzer (Seahorse Bioscience, Billerica, MA, USA) following the manufacturer's manual. Oligomycin and Rotenone were used as inhibitors and the uncoupler FCCP was used as agonist. The results were calculated and represented as the basal respiration, ATP production, proton leakage, maximal respiration and spare capacity.

Flow Cytometry

Flow cytometry were carried out to assess mitochondrial mass using MitoTracker Green FM (MTGFM), a fluorescent mitochondrion-selective probe (Invitrogen,#M7514, USA). S-MSCs were seeded at a density of 4×10^5 cells per well on 12-well plates. After BAs differentiation, cells were suspended by 0.125% trypsin, centrifuged, washed with PBS twice and stained with 100 nM MTGFM at 37℃ for 30 minutes. Then the cells were washed with PBS and followed by staining with Propidium Iodide at room temperature for 15 minutes to label the dead cells. The intensity of fluorescence was measured on a Beckman Coulter CytoFLEX instrument and the mean fluorescence intensity (MFI) was analyzed using a FlowJo 10.2 software.

The following antibodies were used to characterize S-MSCs by flow cytometry: rat anti-mouse CD105-FITC (MJ718, Abcam, #ab184667), rat anti-Mouse CD90-APC (R&D, # FAB7335A), rat anti-mouse CD45-APC (Biolegend, #103112), rat anti-mouse CD140a-PE (PDGFRα, Biolegend, #135906). APC goat anti-rat

IgG2b, FITC goat anti-rat IgG1 and PE goat anti-rat IgG1 (all from BD Bioscience) were used as isotype controls. The gray curves indicate the corresponding negative mouse IgG1 or IgG2a control antibodies.

RNA Extraction and Real-time RT-PCR

S-MSCs were plated at a density of 4×10^5 cells per well on 12-well plates for total RNA extraction. Total RNA was extracted with TRIzol reagent (Gibco Life Technologies) following the manufacturer's manual. Total RNA (2 μg) was reversely transcribed (RT) to cDNA and 0.5 μl RT product was used for Real-time RT-PCR to determine the mRNA level of each gene. Real-time RT-PCR was performed on a StepOnePlus Real-Time PCR System (Applied Biosystems, USA) using the SYBR Green PCR Master Mix (TaKaRa). β-actin was used as internal control. All gene expression results were normalized to the house keeping gene β-actin expression. Cycle threshold (CT) was used for data analysis. All cytokines primers were ordered from Invitrogen (Shanghai). The Primers sequences were listed as follows: PPARG coactivator 1 alpha (PGC-1α): (sense: 5'-CCCTGCCATTGTTAAGACC-3', antisense: 5'-TGCTGCTGTTCCTGTTTTC-3'); uncoupling protein 1 (UCP-1): (sense: 5'-ACTGCCACACCTCCAGTCATT-3', antisense: 5'-CTTTGCCTCACTCAGGATTGG-3'); nuclear respiratory factor 1 (NRF1): (sense: 5'-GCCGTCGGAGCACTTACT-3', antisense: 5'-CTGTTCCAATGTCACCACC-3'); transcription factor A (TFAM): (sense: 5'-CGCAGCACCTTTGGAGAA-3', antisense: 5'-CCCGACCTGTGGAATACTT-3') .

Immunoblotting

S-MSCs were plated at a density of 8×10^5 cells per well on 6-well plates. After BAs differentiation, cells were lysed in cell lysis buffer (10 mmol/L Tris-HCl PH7.5, 150 mmol/L NaCl, 0.1% SDS, 1%TritonX-100, 2μ g/ml Aprotinin, 2μ g/ml Leupeptin and 1 mmol/L PMSF) (Beyotime, Shanghai, China). Protein concentrations were determined using the bicinchoninic acid protein assay (Thermo Fisher Scientific). Aliquots containing 10μ g of total protein were subjected to SDS-PAGE in 12% gels for Western blotting (WB) with antibodies: anti-PGC1-α antibody (Abcam, #ab54481, 1:1000 dilution), anti-UCP-1 antibody ((Abcam, #ab10983, 1:1000 dilution), mitochondrial complex-1 (Proteintech, #15181-1-AP, 1:4000 dilution) and complex-4 antibodies ((Proteintech, #26003-1-AP, 1:2500 dilution), anti-GAPDH (Proteintech, HRP-60004, dilution: 1:4000). Ang II-stimulated brown adipocytes either induced from S-MSCs or isolated from iBAT of mice were lysed in cell lysis buffer and collected for WB with anti-PGC1-α, anti-UCP-1, and anti-GAPDH antibodies. All the PVDF membranes (Millipore Sigma) were incubated with horseradish peroxidase-conjugated secondary antibodies: goat anti-mouse IgG (Proteintech, #SA00001-1, 1:5000 dilution), goat anti-rabbit IgG (Proteintech,#SA00001-2, 1:5000 dilution) for 2 hours. The immunoreactive bands were detected using an enhanced chemiluminescence detection kit (Perkin Elmer). The immunoblot bands were quantified by densitometry.

Hypertension induction and blood pressure measurement

Minipumps (1004, Alzet, Cupertino, California) were implanted subcutaneously in mice to deliver Ang II (Sigma) or 0.9% NaCl. Blood pressure (BP) was measured by tail-cuff using the BP-2000 Blood Pressure Analysis System (Visitech Systems, Napa Place Apex, North Carolina). Starting from 10 weeks of age, 12 male C57BL/6 mice were randomly divided into 2 groups: WT-C (Control group, infused with 0.9% NaCl, n

= 6), WT-A (Ang II-infused group, infused with Ang II for 28 days- 750 ng/kg per minute, n = 6), this induction is only for investigating change of interscapular brown adipose tissue (iBAT) to white adipose tissue (WAT) in angiotensin II(Ang II)-induced hypertensive mice. Starting from 10 weeks of age, 24 male C57BL/6 mice were randomly divided into 4 groups respectively: WT-C (infused with 0.9% NaCl), -BAT-34-C (iBAT-deficiency mice infused with 0.9% NaCl, the iBAT depot were surgically removed and allowed to recover for 6 days, and then treated with 0.9% NaCl for another 28 days), WT-Ang II (infused with 750 ng/kg per minute Ang II for 28 days), -BAT-34-Ang II (iBAT-deficiency mice infused with Ang II, the iBAT depot were surgically removed and allowed to recover for 6 days, and then treated with 750 ng/kg per minute Ang II for 28 days). Noninvasive tail-cuff monitoring of systolic blood pressure (SBP) of above 4 groups of mice (n = 6).

Histological Analysis

Aorta, iBAT or heart tissue fixed by Paraformaldehyde was embedded in paraffin and 6-μm sections were stained with hematoxylin and eosin (HE) staining [13]. Images of tissues were obtained by using the Axio Imager 2 upright microscope (Zeiss, Germany), and the images were acquired with ZEN Imaging software (Zeiss, Germany). Mitochondrional staining: S-MSCs were plated at a density of 2×10^4 per well on 48-well plates. Mitochondria of undifferentiated and differentiated 4 days of S-MSCs were stained with 200 nM MitoTracker Red CMXRox (Invitrogen, #M7512) at 37℃ for 30 minutes. Nuclei of the cells were stained with DAPI. The fluorescent images were captured by Axio invert microscope (Zeiss, Germany).

Statistical Analysis

The data were analyzed with GraphPad Prism 5 and were presented as the mean ± SD. Student's t-test was used when two conditions were compared, and analysis of variance (ANOVA) with Bonferroni or Newman-Keuls correction was used for multiple comparisons. Probability values of < 0.05 were considered significant; two-sided Student's t-tests or ANOVA were performed. *p<0.05; **p<0.01; ***p < 0.001; ****p < 0.0001; ns, not significant. Error bars depicted SD.

Results

PDGFRα $^+$ S-MSCs readily differentiated into brown-type adipocytes in vitro

BAs are known to be derived from the multipotent progenitor cells, such as PDGFRα$^+$ ASCs [10]. S-MSCs are a type of easily attainable MSCs recently favored in stem cell research and the development of tissue therapies [12–15]. We reasoned that, S-MSCs could also be induced to differentiate into BAs. Here, we demonstrated that S-MSCs isolated from the dermis of mouse skin expressed the stem cell markers CD90/105 and PDGFRα by FACS analysis **(Fig. 1A)**. In order to initiate BA induction, S-MSCs were stimulated with an adipogenic cocktail containing insulin, IBMX, dexamethasone, triiodothyronine (T3), and rosiglitazone for the indicated periods. Lipid droplets became discernible in the cells with 2 days of stimulation and could be observed in about 90% of the cells by day 8, indicating the transition of the cells into BAs **(Fig. 1B)**. Thermogenic markers mitochondrial UCP-1 and PGC-1α have been dubbed the

hallmark of BAs [9]. We measured the expression of UCP-1 and PGC-1α in the cells during the course of induced differentiation by RT-PCR and found that the levels of UCP-1 and PGC-1α transcripts steadily increased during the 10-day period of differentiation, with a slight drop in PGC-1α level at day10 **(Fig. 1C)**. This mRNA expression pattern was largely correlated with their protein levels during differentiation, in which both markers showed a continual increase with a minor drop on day 10 **(Fig. 1D)**. These results showed that S-MSCs expressed PDGFRα and readily differentiated into BAs upon adipogenic induction *in vitro*.

BA differentiation of S-MSCs is accompanied by enhanced oxygen consumption

Increased mitochondrial activity is a prerequisite for MSC differentiation into adipocytes [17]. Using the Seahorse XFe96 analyzer, we found that oxygen consumption of S-MSCs was highly increased during the differentiation periods from day 2 to day 8 **(Fig. 2A)**, indicating that BA differentiation of S-MSCs is a process that requires enhanced mitochondrial function and energy supply. Mitochondrial function as indicated by ATP levels and mitochondrial complex activities such as basal mitochondrial respiration, proton leak, maximal respiratory capacity, and spare capacity were also significantly enhanced during the adipogenic differentiation process **(Fig. 2B-F)**, suggesting that S-MSCs not only acquire higher baseline oxygen consumption, but also exhibit more activated mitochondrial function during BA differentiation.

Mitochondrial biogenesis was increased during BA differentiation of S-MSCs

To further examine the role of mitochondria in brown adipogenic differentiation of S-MSCs, we measured mitochondrial mass in the S-MSCs stimulated with brown adipogenic cocktail for the indicated times by staining with MTGFM and subsequent analysis by flow cytometry. Results demonstrated that mitochondrial mass was significantly increased in the S-MSCs after 2 days of BA differentiation and remained at a relatively high level throughout the BA differentiation process **(Fig. 3A)**. Consistently, fluorescence microscopy of cells stained with MTGFM and DAPI also showed the increased mitochondrial content in cells at day 4 after stimulation compared with unstimulated S-MSCs **(Fig. 3B).** Immunoblot analysis showed that expression of mitochondrial complex-1 and complex-4 proteins was robustly enhanced during the BA differentiation process **(Fig. 3C)**. Further, real-time RT-PCR revealed that the mRNA levels of mitochondrial TFAM and NRF1, the key regulating factors of mitochondrial biogenesis, were up-regulated significantly during the BA differentiation of S-MSCs **(Fig. 3D)**. These data confirmed that the mitochondrial biogenesis is boosted during the BA differentiation of S-MSCs.

Change of interscapular brown fat tissue to white fat tissue in Ang II-induced hypertensive mice

BAT is mainly composed of BAs. Animal studies has displayed that transgenic ablation of BAT is associated with systemic hypertension [3]. However, the change of BAT in Ang II-induced hypertensive mice is rarely investigated. Here, we employed the Ang II-induced hypertensive mouse model. During 28 days of Ang II infusion at 750 ng/kg/min administered by ALZET osmotic pumps, the Ang II-infused mice showed a significant increase of systolic blood pressure (SBP) as well as remarkable vascular injury compared with the control mice **(Fig. 4A and 4B).** Subsequent histological analysis revealed extensive

brown-to-white adipose transformation in the iBAT extracted from the Ang II-infused mice compared with the control mice **(Fig. 4C)**. For further *in vitro* assessment, we used Ang II to stimulate BAs either induced from S-MSC differentiation or isolated from the iBAT of mice, and found that expression of brown fat-specific marker UCP-1 and adipogenic marker PGC-1α was decreased in a dose-dependent manner after Ang II stimulation **(Fig. 4D and 4E)**. Together, these data suggest that Ang II causes the whitening of BAT in hypertensive mice and induced BA dysfunction *in vitro*.

Brown adipose tissue-deficiency enhanced Ang II-induced hypertension and vascular remodeling

Prompted by these results, we next aimed to determine the direct role of BAT in blood pressure (BP) regulation by using iBAT-deficient mice (generated by surgically removing the iBAT depot in C57BL/6 mice and allowing to recover for 6 days, -BAT) and WT mice. At day 7, -BAT and WT mice were further administered Ang II or 0.9% NaCl infusion at 750 ng/kg per minute for 28 days and BP was monitored using the noninvasive tail cuff method. We found that iBAT-deficient mice manifested drastically increased SBP elevation compared with WT mice **(Fig. 5A)**. The histological analysis of aorta sections was used to examine the aorta structural changes, and HE staining showed that 4 weeks of Ang II infusion caused hypertrophy of aortas (intima and media), which was aggravated in iBAT-deficient mice **(Fig. 5B)**. The aortic intima and media thickness were quantified **(Fig. 5C)**. Ang II-induced fibrosis of heart was significantly aggravated in iBAT-deficient mice compared with WT mice **(Fig. 5D)**. Collectively, these data suggested that the direct deficiency of iBAT was able to facilitate Ang II-induced BP elevation and target organ damage.

Discussion

The ability, molecular mechanism and role of the differentiation of S-MSCs into BAs have not been demonstrated before. Although it is well documented that BAs are derived from distinct developmental origins, such as PDGFRα$^+$ ASCs located in WAT that express the common stem cell markers Sca1 and are shown to differentiate into BAs *in vitro* and *in vivo* [10]. BAs play a key role in the endocrine protection of hypertensive cardiac remodeling by activating A2AR/FGF21 pathway [5]. In the present study, we revealed that S-MSCs isolated in the dermis of mouse skin which expressed PDGFRα and readily differentiated into BAs regulated by mitochondrial activity *in vitro.* S-MSCs could be another promising developmental origin of BAs. Functionally, Ang II causes the iBAT to turn into WAT in Ang II-induced hypertensive mice and decreased the thermogenic functional genes UCP-1 and PGC-1α expression *in vitro*. The direct deficiency of iBAT markedly facilitated Ang II–induced BP elevation and target organ damage.

Recent studies have revealed that BAs could be derived from the Myf5$^+$ progenitor cells located in the perirenal and interscapular regions [21], the Sca-1$^+$ adipogenic progenitor cells residing in murine skeletal muscle and subcutaneous white fat after bone morphogenetic protein 7 (BMP7) stimulation [22]. The BAs emerging in white fat in response to β3-adrenergica stimulation in abdominal WAT that arose from PDGFRα$^+$ ASCs [10]. Human fetal mesenchymal stem cells have been proved to differentiate into BAs [9]. Previous study had confirmed that S-MSCs could migrate to the inflamed tissues and inhibited the

development of atherosclerosis, EAE and hypertension in mouse models, which could be a promising cell source for stem cell-based therapies of chronic inflammatory diseases [12, 13, 15]. To our knowledge, no prior study has addressed the ability of S-MSCs located in the dermis to differentiate into BAs. The present study is the first to demonstrate that S-MSCs are able to readily differentiate into BAs *in vitro*. It could be another promising developmental origin of BAs.

Mitochondria are considered multifaceted organelles that regulate stem cell fate decisions [20]. Generally, mitochondria in MSCs are maintained at a low activity level, and after MSC induction, mitochondrial DNA (mtDNA) copy number, OCR, mitochondrial biogenesis related genes (NRF1 and TFAM) expression and intracellular ATP content are enhanced [23]. Mitochondrial elongation is critical during embryonic stem cell (ESC) differentiation to cardiomyocytes and for the normal cardiac development and function [24]. The robust mitochondrial activity is a prerequisite for hMSC differentiation into adipocytes [17]. The zinc-finger containing protein PRDM16 initiates differentiation of myoblasts or white preadipocytes into functional BAs [7]. The differentiated BAs augment the expression of mitochondrial function genes (NRF1 and TFAM) and ultimately of UCP1 [25]. In agreement with the previous studies described in this article, we found the increased mitochondrial oxygen consumption and expression of thermogenic markers (UCP1 and PGC1-α) and mitochondrial biogenesis markers (NRF1 and TFAM) during BAs differentiation of S-MSCs.

PDGFRα^{+} S-MSCs could be a novel BA progenitors. BAs are the major component of BAT. Transgenic ablation of BAT is associated with cardiovascular abnormalities and systemic hypertension in the UCP-DTA mice [3]. BAT plays a potential endocrine role against hypertensive cardiac remodeling in DOCA-salt induced hypertension [5]. Tissue-grafting of converted BAT has been proposed as a direct approach to increase endogenous brown fat in vivo [26]. In order to directly confirm the role of BAT in AngII-induced hypertension in mice, we firstly detected and compared the changes of iBAT in hypertensive mice to WT control mice, the results showed extensive brown-to-white adipose transformation in the iBAT extracted from the Ang II-infused mice but no change in the control mice. And *in vitro*, we also found that Ang II stimulation caused the decreased expression of UCP-1 and PGC-1α in BAs. Further, we generated iBAT-deficient mice by surgically removing the iBAT depot in C57BL/6 mice followed with Ang II infusion, and the results demonstrated that the direct deficiency of iBAT was able to accelerate Ang II–induced BP elevation and target organ damage compared to control. Overall, this study provides direct evidence that BAT plays a pivotal role in Ang II-induced hypertension and target organ remodeling and further supports previous studies [3, 5].

In conclusion, we provide direct evidence that S-MSCs have a potential ability to easily differentiate into BAs, which is regulated by mitochondrial activity. Functionally, the combination of our *in vitro* and *in vivo* experiments illustrate that Ang II causes the whitening of the iBAT in hypertensive mice and the dysfunction of BAs. And the direct deficiency of iBAT markedly facilitated Ang II–induced BP elevation and target organ damage **(Fig. 6)**. Our results suggest that S-MSCs can readily differentiate into BAs which are potential therapeutic cell type for the treatment of hypertension.

Abbreviations

Skin-derived Mesenchymal Stem Cells (S-MSCs); Brown adipocytes (BAs); Brown adipose tissue (BAT); Adipose-derived stem cells (ASCs); interscapular brown adipose tissue (iBAT); white adipose tissue (WAT); oxygen consumption rate (OCR); angiotensin II (Ang II); Fibroblast growth factor 21 (FGF21); real-time quantitative PCR (RT-PCR); MitoTracker Green FM (MTGFM); mean fluorescence intensity (MFI); uncoupling protein 1 (UCP-1); PPARG coactivator 1 alpha (PGC-1α); nuclear respiratory factor 1 (NRF1); transcription factor A (TFAM).

Declarations

ACKNOWLEDGEMENTS

Not applicable.

AUTHOR CONTRIBUTIONS

Q.L.: study design, collection and/or assembly of data, data analysis, manuscript wri.ting; W.X, W.C and W.S.: perform experiments, collection and/or assembly of data, data analysis; X.L: perform experiments; P.G. and Z.S: manuscript revision.

FUNDING

This research was supported by grants from the Natural Science Foundation of Shanghai Science and Technology Committee (No. 20ZR1447400, No. 16ZR 1429300).

AVAILABILITY OF DATA AND MATERIALS

Not applicable.

ETHICS APPROVAL AND CONSENT TO PARTICIPATE

All mice were kept under specific pathogen-free (SPF) conditions in compliance with the National Institutes of Health Guide for the Care and Use of Laboratory Animals with the approval (SYXK-2003-0026) of the Scientific Investigation Board of Shanghai Jiao Tong University School of Medicine, Shanghai, China. All procedures of animal experiments followed the Guidelines for The Care and Use of Experimental Animals published by the National Institutes of Health, and all efforts are made to minimize animals suffering.

CONSENT FOR PUBLICATION

Not applicable.

COMPETING INTERESTS

The authors declare that they have no competing interests.

AUTHOR DETAILS

[a] The Department of Cardiovascular Medicine, State Key Laboratory of Medical Genomics, Shanghai Key Laboratory of Hypertension, Ruijin Hospital, Shanghai Institute of Hypertension, Shanghai Jiao Tong University School of Medicine, Shanghai, 200025, China

[b] Department of digestion, Huaihe Hospital of Henan University, Kaifeng, 475000, China.

References

1. Cinti, S., *Between brown and white: novel aspects of adipocyte differentiation.* Ann Med, 2011. **43**(2): p. 104-15.
2. Rui, L., *Brown and Beige Adipose Tissues in Health and Disease.* Compr Physiol, 2017. **7**(4): p. 1281-1306.
3. Cittadini, A., et al., *Cardiovascular abnormalities in transgenic mice with reduced brown fat: an animal model of human obesity.* Circulation, 1999. **100**(21): p. 2177-83.
4. Lowell, B.B., et al., *Development of obesity in transgenic mice after genetic ablation of brown adipose tissue.* Nature, 1993. **366**(6457): p. 740-2.
5. Ruan, C.C., et al., *A2A Receptor Activation Attenuates Hypertensive Cardiac Remodeling via Promoting Brown Adipose Tissue-Derived FGF21.* Cell Metab, 2018. **28**(3): p. 476-489 e5.
6. Fu, M., et al., *Neural Crest Cells Differentiate Into Brown Adipocytes and Contribute to Periaortic Arch Adipose Tissue Formation.* Arterioscler Thromb Vasc Biol, 2019. **39**(8): p. 1629-1644.
7. Seale, P., et al., *PRDM16 controls a brown fat/skeletal muscle switch.* Nature, 2008. **454**(7207): p. 961-7.
8. Pittenger, M.F., et al., *Multilineage potential of adult human mesenchymal stem cells.* Science, 1999. **284**(5411): p. 143-7.
9. Morganstein, D.L., et al., *Human fetal mesenchymal stem cells differentiate into brown and white adipocytes: a role for ERRalpha in human UCP1 expression.* Cell Res, 2010. **20**(4): p. 434-44.
10. Lee, Y.H., et al., *In vivo identification of bipotential adipocyte progenitors recruited by beta3-adrenoceptor activation and high-fat feeding.* Cell Metab, 2012. **15**(4): p. 480-91.
11. Bartsch, G., et al., *Propagation, expansion, and multilineage differentiation of human somatic stem cells from dermal progenitors.* Stem Cells Dev, 2005. **14**(3): p. 337-48.
12. Ke, F., et al., *Autocrine Interleukin-6 Drives Skin-Derived Mesenchymal Stem Cell Trafficking via Regulating Voltage-Gated Ca2+ Channels.* STEM CELLS, 2014. **32**(10): p. 2799-2810.
13. Li, Q., et al., *Skin-Derived Mesenchymal Stem Cells Alleviate Atherosclerosis via Modulating Macrophage Function.* Stem Cells Transl Med, 2015.

14. Ke, F., et al., *Soluble Tumor Necrosis Factor Receptor 1 Released by Skin-Derived Mesenchymal Stem Cells Is Critical for Inhibiting Th17 Cell Differentiation.* Stem Cells Transl Med, 2016. **5**(3): p. 301-13.
15. Li, X., et al., *Transplantation of skin mesenchymal stem cells attenuated AngII-induced hypertension and vascular injury.* Biochemical and Biophysical Research Communications, 2018. **497**(4): p. 1068-1075.
16. Tormos, K.V., et al., *Mitochondrial complex III ROS regulate adipocyte differentiation.* Cell Metab, 2011. **14**(4): p. 537-44.
17. Zhang, Y., et al., *Mitochondrial respiration regulates adipogenic differentiation of human mesenchymal stem cells.* PLoS One, 2013. **8**(10): p. e77077.
18. Cho, E., et al., *Cluh plays a pivotal role during adipogenesis by regulating the activity of mitochondria.* Sci Rep, 2019. **9**(1): p. 6820.
19. Shyh-Chang, N., G.Q. Daley, and L.C. Cantley, *Stem cell metabolism in tissue development and aging.* Development, 2013. **140**(12): p. 2535-47.
20. Bahat, A. and A. Gross, *Mitochondrial plasticity in cell fate regulation.* J Biol Chem, 2019. **294**(38): p. 13852-13863.
21. Sanchez-Gurmaches, J. and D.A. Guertin, *Adipocytes arise from multiple lineages that are heterogeneously and dynamically distributed.* Nat Commun, 2014. **5**: p. 4099.
22. Schulz, T.J., et al., *Identification of inducible brown adipocyte progenitors residing in skeletal muscle and white fat.* Proc Natl Acad Sci U S A, 2011. **108**(1): p. 143-8.
23. Li, Q., et al., *The role of mitochondria in osteogenic, adipogenic and chondrogenic differentiation of mesenchymal stem cells.* Protein Cell, 2017. **8**(6): p. 439-445.
24. Kasahara, A., et al., *Mitochondrial fusion directs cardiomyocyte differentiation via calcineurin and Notch signaling.* Science, 2013. **342**(6159): p. 734-7.
25. Bargut, T.C., M.B. Aguila, and C.A. Mandarim-de-Lacerda, *Brown adipose tissue: Updates in cellular and molecular biology.* Tissue Cell, 2016. **48**(5): p. 452-60.
26. Blumenfeld, N.R., et al., *A direct tissue-grafting approach to increasing endogenous brown fat.* Sci Rep, 2018. **8**(1): p. 7957.

Figures

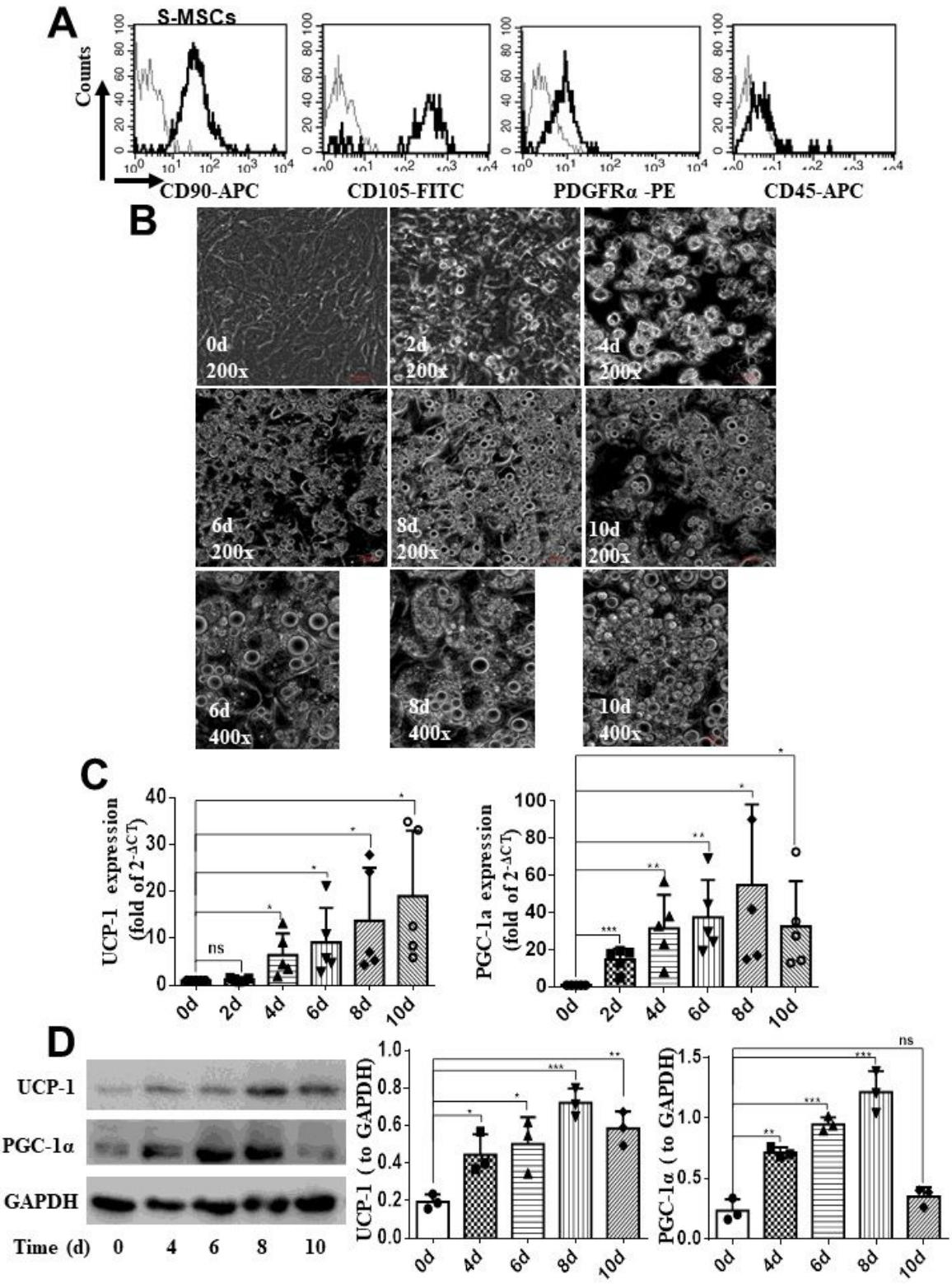

Figure 1

Differentiation of PDGFRα+ S-MSCs into brown adipocytes (BAs) in vitro. S-MSCs were isolated from the dermis of neonatal mice. (A) Phenotypic characteristics of S-MSCs was examined by flow cytometry with antibodies against CD90-PE, CD105-PE, PDGFRα-PE and CD45-PE, the gray curves indicate the corresponding negative IgG control antibodies, respectively. S-MSCs were induced to differentiate for 2, 4, 6, 8, and 10 days by the adipogenic cocktail containing insulin, IBMX, dexamethasone, triiodothyronine

(T3), and rosiglitazone: (B) Images of cells were obtained at 0, 2, 4, 6, 8, and 10 days after stimulation by light microscopy. Original magnifications 100x or 400x. mRNA level (C) and protein expression (D) of PGC-1α and UCP-1 after stimulation of S-MSCs with the adipogenic cocktail were tested by Real-time polymerase chain reaction (RT-PCR) or Western immunoblots (WB), respectively. Densitometric scanning of three WB is quantified in the bar graphs. The results shown are representative of at least three independent experiments. One-way ANOVA (C and D), data passed the normality test. *P<0.05, **P<0.01, ***P<0.001.

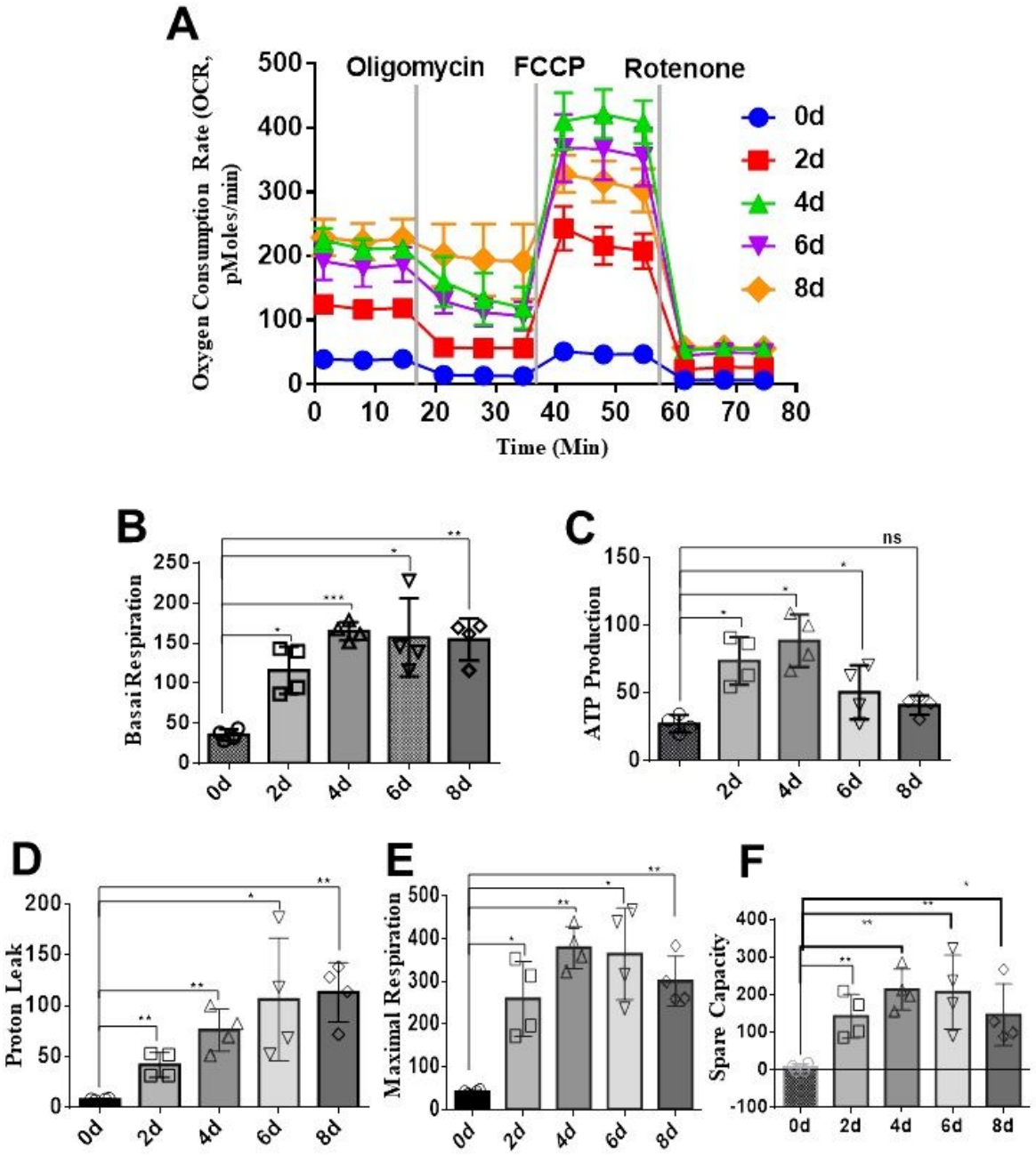

Figure 2

Increased mitochondrial oxygen consumption in brown adipocyte differentiation of S-MSCs. S-MSCs were induced to differentiate for the indicated periods of time (0, 2, 4, 6, and 8 days) with the brown adipogenic cocktail. (A) The oxygen consumption rate (OCR) of S-MSCs at various time points after initial stimulation was measured with an XF24 Extracellular Flux Analyzer (d) experiment program and (e) statistical analysis. Mitochondrial function of the differentiated S-MSCs represented by basal mitochondrial respiration (B), ATP production (C), proton leak (D), maximal respiratory capacity (E), and spare capacity (F). Data are showed as the mean±S.E.M. from at least three independent experiments. One-way ANOVA, *P<0.05, **P<0.01, ***P<0.001 versus relative control.

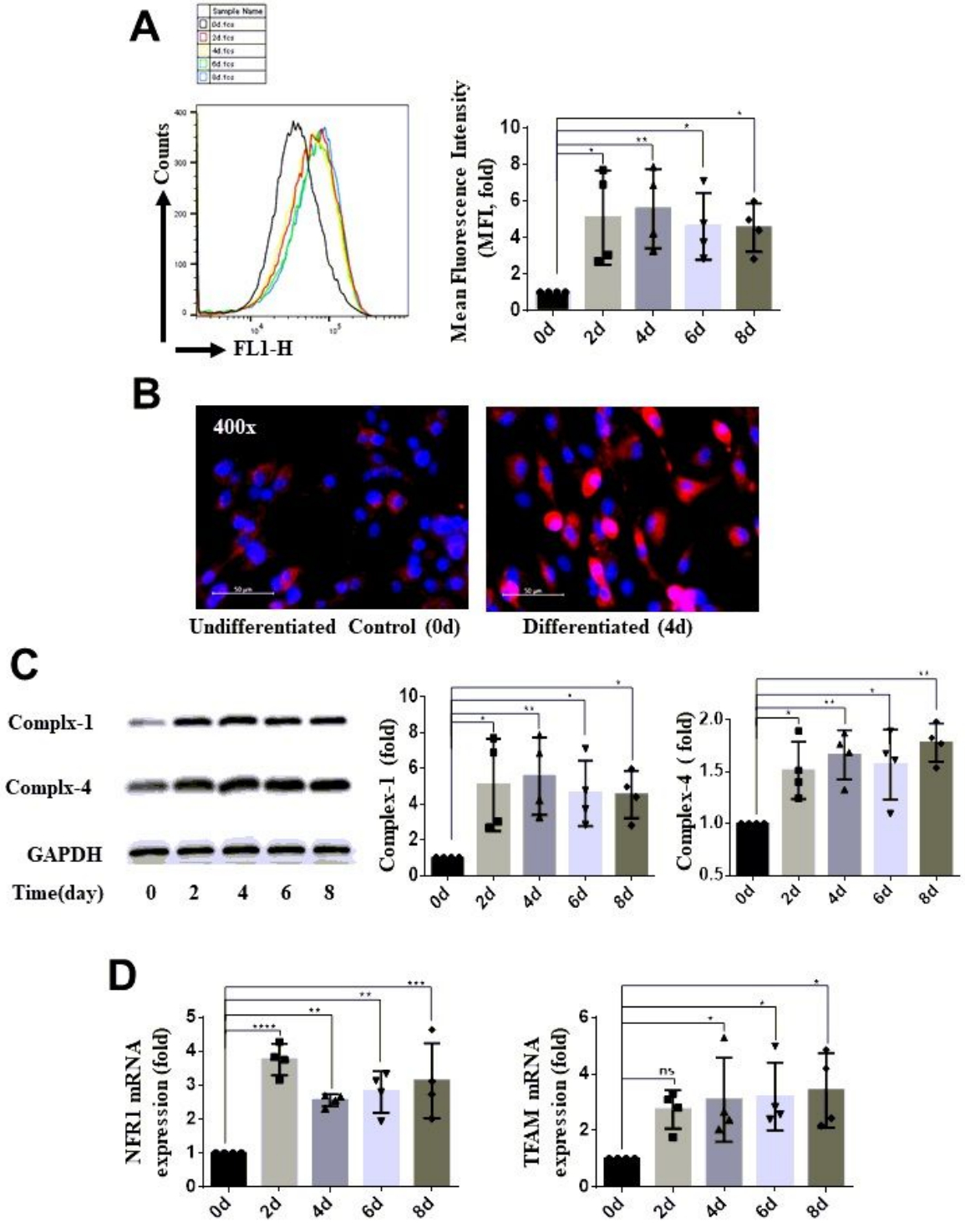

Figure 3

Enhanced mitochondrial biogenesis during brown adipocyte differentiation of S-MSCs. S-MSCs were induced to differentiate for the indicated periods of time. (A) The cells were stained with MitoTracker Green FM (MTGFM) and analyzed by flow cytometry to measure the mitochondrial mass as the mean fluorescence intensity (MFI). (B) Undifferentiated (0d) and differentiated 4 days (4d) of S-MSCs were stained with MitoTracker red and DAPI and visualized by fluorescence microscopy. Original

magnifications 400x. (C) Mitochondrial complex-1 and complex-4 protein expression was tested by WB in cells under differentiation conditions for the indicated time. Densitometric scanning of three WB is quantified in the bar graphs. The results shown are representative of three independent experiments. (D) mRNA levels of mitochondrial transcription factor A (TFAM) and nuclear respiratory factor 1 (NRF1) was investigated by RT-PCR in cells under differentiation conditions for the indicated time. Data are showed as the mean±S.E.M. from at least three independent experiments. One-way ANOVA, *P<0.05, **P<0.01, ***P<0.001 versus relative control.

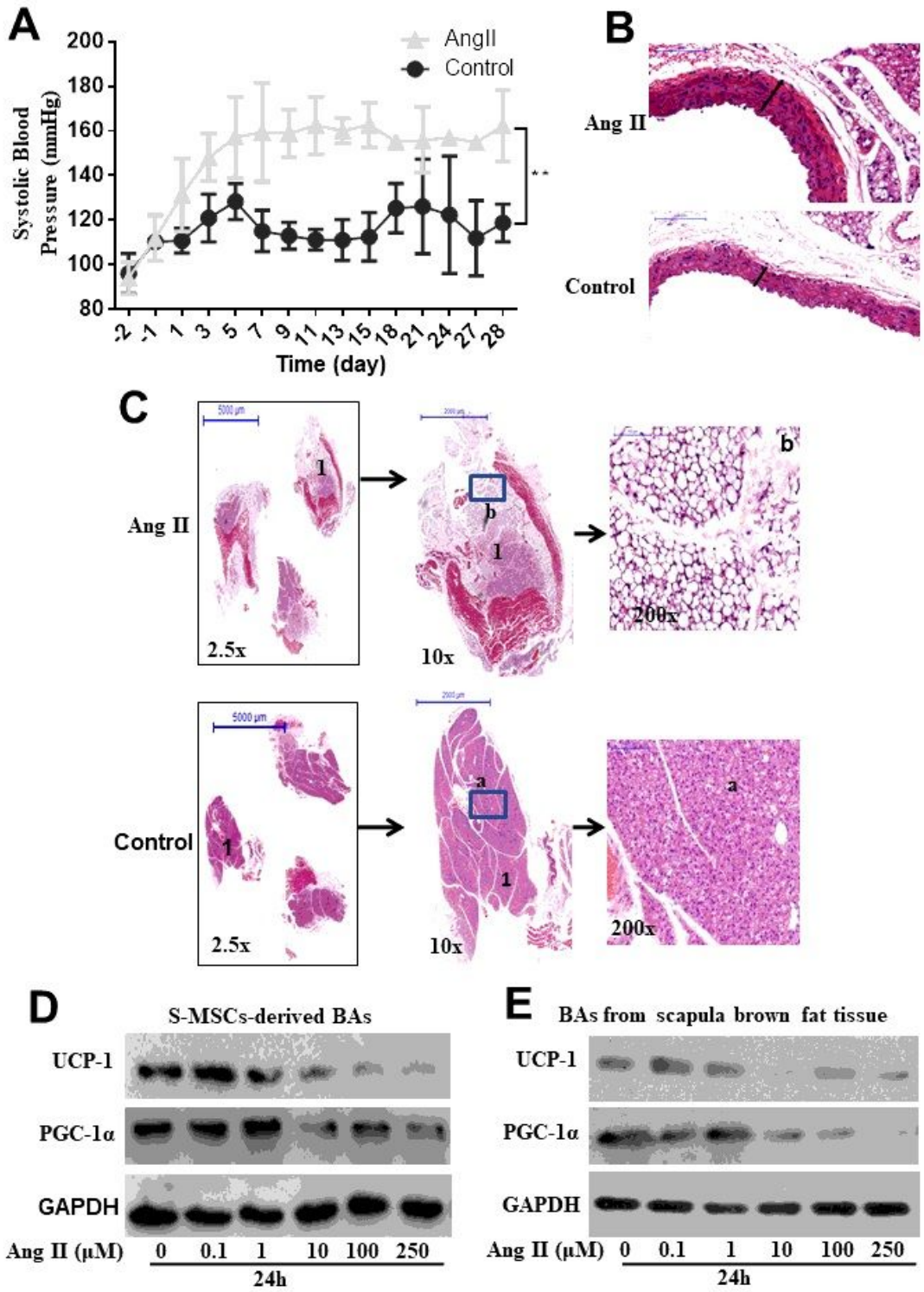

Figure 4

Change of interscapular brown adipose tissue (iBAT) to white adipose tissue (WAT) in angiotensin II (Ang II)-induced hypertensive mice. We constructed hypertensive mouse models in C57BL/6 (wild-type, WT) mice (750 ng/kg per minute Ang II infusion for 28 days, AngII group, and infusion with 0.9% NaCl, Control group). (A) Noninvasive tail-cuff monitoring of systolic blood pressure (SBP) of above 2 groups of mice. (B) Representative HE staining of aortic sections and showing of aortic intima and media thickness (n=4). (C) Representative HE staining of iBAT sections and showing the change of BAT to WAT in iBAT from above 2 groups of mice. Immunoblotting analysis of UCP-1 and PGC-1α protein expressions in Ang II-stimualted brown adipocytes either induced from S-MSCs (D) or isolated from iBAT of mice (E).

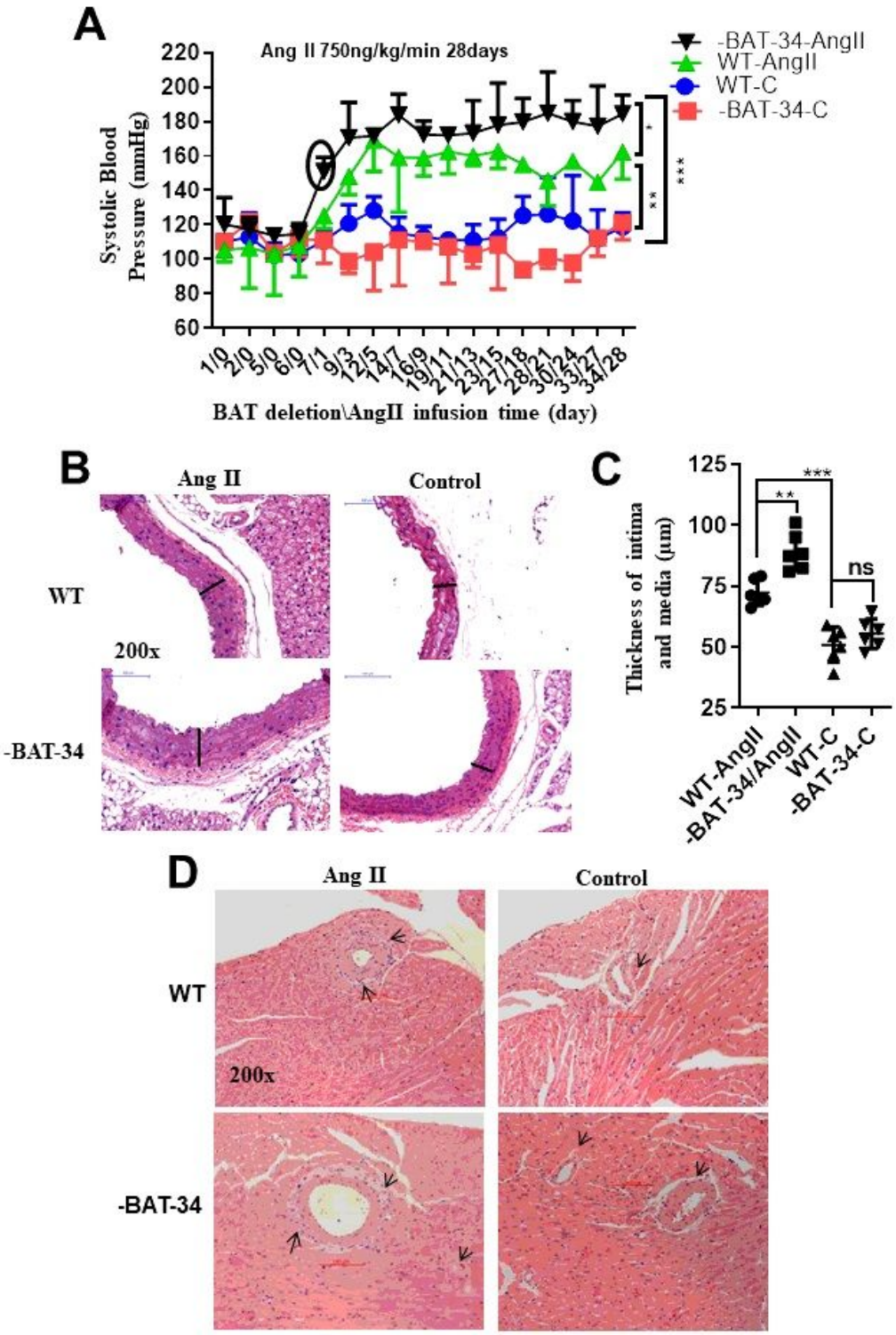

Figure 5

Brown adipose tissue-deficiency enhanced angiotensin II (Ang II)-induced hypertension and target organs remodeling. We constructed hypertensive mouse model (750 ng/kg per minute Ang II or 0.9% NaCl infused for 28 days) in C57BL/6 mice and built 4 groups : WT-C (infused with 0.9% NaCl), -BAT-34-C (iBAT-deficiency mice infused with 0.9% NaCl), WT-Ang II (infused with Ang II), -BAT-34-Ang II (iBAT-deficiency mice infused with Ang II). (A) Noninvasive tail-cuff monitoring of systolic blood pressure (SBP) of above

4 groups of mice (n=5–6). (B, C) Representative HE staining of aortic sections and quantification of aortic intima and media thickness (n=4). (D) Representative HE staining of heart sections (fibrotic tissues showed with arrow) (n=4).

Supplementary Files

This is a list of supplementary files associated with this preprint. Click to download.

- Onlinerenamed3c7fc.Png